

Successive-Cancellation Flip Decoding of Polar Codes with a Simplified Restart Mechanism

Ilshat Sagitov*, Charles Pillet*, Alexios Balatsoukas-Stimming[†], and Pascal Giard*

*Department of Electrical Engineering, École de technologie supérieure, Montréal, Québec, Canada.

Email: {ilshat.sagitov.1, charles.pillet.1}@ens.etsmtl.ca, pascal.giard@etsmtl.ca

[†]Department of Electrical Engineering, Eindhoven University of Technology, Eindhoven, The Netherlands.

Email: a.k.balatsoukas.stimming@tue.nl

Abstract—Polar codes are a class of error-correcting codes that provably achieve the capacity of practical channels. The successive-cancellation flip (SCF) decoder is a low-complexity decoder that was proposed to improve the performance of the successive-cancellation (SC) decoder as an alternative to the high-complexity successive-cancellation list (SCL) decoder. The SCF decoder improves the error-correction performance of the SC decoder, but the variable execution time and the high worst-case execution time pose a challenge for the realization of receivers with fixed-time algorithms. The dynamic SCF (DSCF) variation of the SCF decoder further improves the error-correction performance but the challenge of decoding delay remains. In this work, we propose a simplified restart mechanism (SRM) that reduces the execution time of SCF and DSCF decoders through conditional restart of the additional trials from the second half of the codeword. We show that the proposed mechanism is able to improve the execution time characteristics of SCF and DSCF decoders while providing identical error-correction performance. For a DSCF decoder that can flip up to 3 simultaneous bits per decoding trial, the average execution time, the average additional execution time and the execution-time variance are reduced by approximately 31%, 37% and 57%, respectively. For this setup, the mechanism requires approximately 3.9% additional memory.

I. INTRODUCTION

Polar codes [1] are a type of linear error-correction codes which can achieve the channel capacity for practically relevant channels under low-complexity successive-cancellation (SC) decoding. However, at short to moderate block lengths, the SC algorithm provides an error-correction performance that is lacking for many practical applications. To address this, the successive-cancellation list (SCL) decoding algorithm was proposed [2]. It provides great error-correction capability to the extent that polar codes were selected to protect the control channel in 3GPP’s next-generation mobile-communication standard (5G), where SCL serves as the error-correction performance baseline [3]. However, the error-correction capability of the SCL decoder comes at the cost of high hardware implementation complexity and low energy efficiency [4].

As an alternative to SCL decoding, the successive-cancellation flip (SCF) decoding algorithm was proposed [5]. SCF leads to an improved error-correction performance compared to SC, but still falls behind the SCL decoder with a moderate list size. However, the SCF decoder is more efficient than SCL both in terms of computing resources and energy requirements [6]. Dynamic SCF (DSCF) decoding, proposed in [7], significantly improves the error-correction performance

of SCF decoding. DSCF implements a better metric to identify bit-flipping candidates and the multiple bit-flipping methodology. Preliminary results from a hardware implementation indicate that DSCF decoders have a higher energy efficiency compared to SCL decoders with moderate list sizes while providing similar error-correction performance [8].

Both SCF and DSCF decoders exhibit a variable execution time and the variance of that execution time can be significant. This poses a challenge in the realization of receivers, where fixed-time algorithms are preferred. An early-stopping mechanism for the single bit-flip DSCF decoder that aims to reduce the execution-time characteristics was proposed in [9]. However, it negatively affects the error-correction performance.

Contributions: In this work, we propose a simplified restart mechanism (SRM) that reduces the average execution time, the average additional execution time and the execution-time variance of SCF and DSCF decoders for polar codes. The central idea of the mechanism is to conditionally restart additional decoding trials from the second half of the codeword by using computations stored following the initial SC pass. The error-correction performance is identical to the original non-SRM decoders. For the multi bit-flip version of DSCF, the average execution time, the average additional execution time and the execution-time variance are reduced by 31–58%, while the additional memory overhead is 2.9–3.9%.

Outline: The remainder of this paper is organized as follows. Section II provides an introduction to polar codes, briefly describes SC, SCF and DSCF decoders. In Section III, the SRM is presented, where an algorithm is described along with memory requirements. In Section IV execution-time characteristics of decoders under hardware constraints are discussed. In Section V, the simulation methodology and results are presented. Section VI concludes the work.

II. BACKGROUND

A. Construction of Polar Codes

A polar code $\mathcal{P}(N, k)$, where $N = 2^n$ is the code length and k is the code dimension, relies on the channel polarization induced by $\mathbf{G}^{\otimes n}$, defined as the n^{th} Kronecker power of the binary kernel $\mathbf{G} = \begin{bmatrix} 1 & 0 \\ 1 & 1 \end{bmatrix}$. The $(N - k)$ least-reliable bits, called frozen bits, are set to predefined values that are known by the decoder, typically all zeros. The k information bits are set to the most reliable positions and the code rate is $R = k/N$.

The encoding is performed as $\mathbf{x} = \mathbf{u}\mathbf{G}^{\otimes n}$, where \mathbf{x} and \mathbf{u} are a codeword and an input vector, respectively. The input vector \mathbf{u} contains the k information bits in their predefined locations as well as the frozen-bit values. We denote the set of frozen bit indices of the input vector by \mathcal{A}^C and the set of information bit indices by \mathcal{A} . The bit-location reliabilities depend on the channel type and conditions. In this work, the additive white Gaussian noise (AWGN) channel is considered and the construction method used is that of Tal and Vardy [10].

B. Successive-Cancellation Decoding

The SC decoding schedule can be represented as a binary tree traversal through the layers $s \in \{0, \dots, n\}$ starting from the root node ($s = n$) with the message passing to the left-hand side (LHS) and then to the right-hand side (RHS) of the decoding tree. The decoding tree of a $\mathcal{P}(8, 4)$ polar code is shown in Fig. 1. The received vector of channel log-likelihood ratios (LLRs), denoted by $\alpha_{\text{ch}} = [\alpha_{\text{ch}}(0), \dots, \alpha_{\text{ch}}(N-1)]$, is at the tree root. The v^{th} intermediate node, located in layer s , having input vector $\alpha_v \in \mathbb{R}^{2^s}$ forwards message $\alpha_l \in \mathbb{R}^{2^{s-1}}$ to its left l and $\alpha_r \in \mathbb{R}^{2^{s-1}}$ to its right r as:

$$\alpha_l(j) = f(\alpha_v(j), \alpha_v(j + 2^{s-1})), \quad (1)$$

$$\alpha_r(j) = g(\alpha_v(j), \alpha_v(j + 2^{s-1}), \beta_l(j)), \quad (2)$$

with $0 \leq j < 2^{s-1}$ and the $f: \mathbb{R}^2 \rightarrow \mathbb{R}$ function is the boxplus operator whose hardware-friendly implementation is:

$$f(a, d) = \text{sign}(a) \cdot \text{sign}(d) \cdot \min(|a|, |d|) \quad (3)$$

and the $g: \mathbb{R}^2 \times \mathbb{F}_2 \rightarrow \mathbb{R}$ function is defined as:

$$g(a, d, b) = (1 - 2b) \cdot a + d. \quad (4)$$

LLRs at the leaf nodes of the tree are called decision LLRs and denoted by $\alpha_{\text{dec}} = [\alpha_{\text{dec}}(0), \dots, \alpha_{\text{dec}}(N-1)]$. Each information bit from the transmitted vector $\hat{\mathbf{u}} = [\hat{u}_0, \dots, \hat{u}_{N-1}]$ is estimated by taking a hard decision on the corresponding decision LLR. Frozen bits are known to the decoder and thus directly estimated. Nodes of decision LLRs corresponding to information bits are in black and of frozen bits are in white in Fig. 1. Bit-estimates are propagated from lower to higher layers of the tree and used for calculations of partial-sums. The vector of partial-sums, denoted by β , is calculated for node v at layer s (Fig. 1) as follows:

$$\beta_v(j) = \begin{cases} \beta_l(j) \oplus \beta_r(j) & \text{if } j < 2^{s-1}, \\ \beta_r(j) & \text{otherwise,} \end{cases} \quad (5)$$

where operator \oplus is bitwise XOR operation.

C. SC-Flip Decoding

The SCF decoding algorithm is introduced in [5], where the authors observed that if the first erroneously-estimated bit could be detected and corrected before resuming SC decoding, the error-correction capability of the decoder would be greatly improved. In order to detect decoding failure of the codeword, information bits are concatenated with a r -bit cyclic-redundancy check (CRC) being passed through the

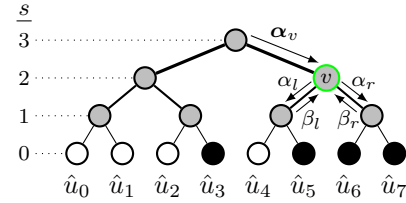


Fig. 1: SC decoding tree of $\mathcal{P}(8, 4)$ polar code.

polar encoder. The CRC bits extend the set of information bits \mathcal{A} of the polar code, increasing the code rate to $R = (k+r)/N$.

If decoding failure is identified at the end of the initial SC decoding pass, a list of bit-flipping candidates, denoted by $\mathcal{B}_{\text{flip}}$, is constructed. The information bit indices with the smallest metrics are identified with the absolute values of α_{dec} being the metrics. The bit-flipping indices are stored in $\mathcal{B}_{\text{flip}}$ in ascending order of their corresponding metrics.

In order to constrain the decoding delay of SCF decoding, the maximum number of trials T_{max} is defined, where $T_{\text{max}} \in \mathbb{N}^+$ and $1 \leq T_{\text{max}} \leq (k+r+1)$, including the initial SC pass. When additional trials are performed, one bit from $\mathcal{B}_{\text{flip}}$ is selected for flipping. Setting $T_{\text{max}} = 1$ renders SCF equivalent to SC decoding. If the CRC fails after T_{max} trials, the decoding is stopped and failure is declared. We highlight that $T_{\text{max}} - 1$ is the total number of flipping candidates.

D. Dynamic SC-Flip Decoding

DSCF decoding is proposed in [7] with two major improvements to original SCF. First, a more accurate metric for constructing $\mathcal{B}_{\text{flip}}$ is derived. Second, a methodology of flipping multiple bits is proposed, i.e., the decoder is able to flip more than one bit per decoding trial.

Flipping of multiple bits is achieved by progressively updating the set of bit-flipping candidates $\varepsilon_t = \{i_\lambda\}$, where t is index of additional trial. The current set size is denoted by λ , $1 \leq \lambda \leq \omega$ and $i_1 \leq i_\lambda \leq i_\omega$. The maximum set size, or decoding order [7], is denoted by ω and indicates the maximum number of bit-flips per trial.

For each bit-flipping set ε_t the metric calculation and update are performed according to:

$$\mathcal{M}_{\text{flip}}(\varepsilon_t) = \sum_{j \in \varepsilon_t} |\alpha_{\text{dec}}(j)| + \Pi(\varepsilon_t), \quad (6)$$

where $\Pi(\varepsilon_t)$ is:

$$\Pi(\varepsilon_t) = \frac{1}{c} \sum_{\substack{j \leq i_\lambda \\ j \in \mathcal{A}}} \ln(1 + e^{-c \cdot |\alpha_{\text{dec}}(j)|}), \quad (7)$$

where $0 < c \leq 1$. The value of c is optimized for different block lengths, rates and channel conditions. Similarly to SCF decoding, each set ε_t is stored in list $\mathcal{B}_{\text{flip}}$ in ascending order of metric $\mathcal{M}_{\text{flip}}(\varepsilon_t)$.

After an initial SC pass with a decoding failure, the bit-flipping candidates are constructed similarly to SCF, but with the metric (7) with $\lambda = 1$. If the maximum set size is $\omega = 1$, no additional metric updates are performed: bit-flipping

candidates are sorted in ascending order of metrics and each bit flip is chosen accordingly for additional decoding trial. If $\omega > 1$, multiple bit flips are applied and each decoding set is updated at every unsuccessful decoding attempt. At each attempt, a new information index is progressively inserted to a temporary constructed set and the metric update is performed for this set. If metric of the temporary set exceeds the largest metric of the list, it is discarded. If not, it is added to the list while keeping the metric list sorted. The set is not extended further after reaching the maximum size ω .

The decoder is called DSCF- ω to emphasize the dependence on the parameter ω . A total of T_{\max} trials are run with a total of $T_{\max} - 1$ bit-flipping sets. Thus, the index of sets is in the range of $1 \leq t \leq T_{\max} - 1$. We highlight that $T_{\max} \geq (k+r+1)$ is applicable when $\omega > 1$, since multiple sets resulting from one single or multi bit-flipping set can be constructed and used as the bit-flipping candidates.

Metric Approximation: The metric Π (7) contains logarithmic and exponential computations. To make the metric updates more hardware-friendly, an approximation is proposed in [11]. We denote it as Π' and it is defined as:

$$\Pi'(\varepsilon_t) = \begin{cases} 1.5, & \text{if } |\alpha_{\text{dec}}(j)| \leq 5.0, \\ 0, & \text{otherwise.} \end{cases} \quad (8)$$

This approximation was shown to result in a negligible coding loss [8], [11]. In the remainder, the approximation Π' is used for the metric calculations and update of DSCF- ω decoding.

III. SIMPLIFIED RESTART MECHANISM

In this section, we describe our proposed simplified restart mechanism (SRM) for SCF and DSCF- ω decoding. The SRM conditionally avoids redundant computations by storing the necessary bits obtained during the first SC pass into an additional memory. This section also provides a memory analysis.

A. Description of the SRM

Each additional trial in SCF decoding (and its variants) starts by redoing the SC computations to estimate the very first information bit, and then proceeds all the way to the location that corresponds to the information bit that needs to be flipped. However, we observe that decoding of both bits \hat{u}_0 and $\hat{u}_{N/2}$ begins from the root layer $s = n$ of the decoding tree, where channel LLRs are used. The latter are constant throughout SCF decoding of the current codeword. Therefore, if the information bit that needs to be flipped is located on the RHS tree, intermediate LLR calculations of the LHS tree can be entirely avoided. These observations are independent from the specific patterns of information and frozen bits. The estimated bits and partial-sum results of the LHS tree are still required for the RHS SC computations.

Due to channel polarization, the information bits are predominantly located at the RHS of the decoding tree. In Fig. 1, $3/4$ of the information bits are on the RHS. Naturally, bit flips in SCF will often occur on the RHS. For each additional trial where the flipping index is on the RHS, we propose to skip the (unchanged) LHS of the decoding tree, i.e., keep the initial

$[\hat{u}_0, \dots, \hat{u}_{N/2-1}]$ and decode $[\hat{u}_{N/2}, \dots, \hat{u}_{N-1}]$. To do so, the LHS computations from the initial SC pass must be available, i.e., the partial sums β_{rest} and estimated bits \hat{u}_{rest} .

Algorithm 1 SCF decoding embedding the SRM.

```

1: procedure SCF_WITH_SRM( $\alpha_{\text{ch}}, \mathcal{A}, T_{\max}$ )
2:    $\beta_{\text{rest}} \leftarrow [0, 0, \dots, 0]$ 
3:    $\hat{u}_{\text{rest}} \leftarrow [0, 0, \dots, 0]$ 
4:    $\psi_{\text{rest}} \leftarrow N/2 - 1$ 
5:   for  $t = 1, t \leq T_{\max}, t = t + 1$  do
6:     if  $t > 1$  then ▷ Only at additional trials
7:       if  $\mathcal{B}_{\text{flip}}(t) > \psi_{\text{rest}}$  then ▷ Activate SRM if needed
8:          $\beta(0, \dots, \psi_{\text{rest}}) \leftarrow \beta_{\text{rest}}$  ▷ Load partial sums
9:          $\hat{u}(0, \dots, \psi_{\text{rest}}) \leftarrow \hat{u}_{\text{rest}}$  ▷ Load bit estimates
10:         $\text{sr}_{\text{m\_act}} \leftarrow \text{True}$  ▷ Set SRM flag
11:      else
12:         $\text{sr}_{\text{m\_act}} \leftarrow \text{False}$  ▷ Reset SRM flag
13:      end if
14:    else
15:       $\text{sr}_{\text{m\_act}} \leftarrow \text{False}$ 
16:    end if
17:     $(\hat{u}, \alpha_{\text{dec}}) \leftarrow \text{SC}(\alpha_{\text{ch}}, \mathcal{A}, \mathcal{B}_{\text{flip}}(t), \beta, \text{sr}_{\text{m\_act}})$ 
18:    if  $\text{CRC}(\hat{u}) = \text{failure}$  then
19:      if  $t = 1$  then ▷ Only at initial trial
20:         $\mathcal{B}_{\text{flip}} \leftarrow \text{Init\_Flip\_Set}(\alpha_{\text{dec}}, T_{\max} - 1)$ 
21:         $\beta_{\text{rest}} \leftarrow \beta(0, \dots, \psi_{\text{rest}})$  ▷ Store partial sums
22:         $\hat{u}_{\text{rest}} \leftarrow \hat{u}(0, \dots, \psi_{\text{rest}})$  ▷ Store bit estimates
23:      else
24:        continue
25:      end if
26:    else
27:      break
28:    end if
29:  end for
30:  return  $\hat{u}$ 
31: end procedure

```

Algorithm 1 summarizes how a version of SCF that embeds our proposed SRM works. The algorithm follows the original course of decoding that was described in Section II-C. When the CRC fails after the initial SC pass, the bit estimates and partial sums are stored into restart lists. The bit-flipping candidates are initialized. If during additional trials the bit-flipping index at the RHS of the tree identified, the SRM flag is raised, stored lists are copied to active lists of β and \hat{u} . The SC decoding is then resumed from the bit $\hat{u}_{N/2}$.

The proposed SRM for DSCF- ω decoding with $\omega = 1$ follows the same decoding schedule as in Algorithm 1 except the use of the metric function that results on different bit-flipping list. For each bit-flipping set $\varepsilon_t = \{i_\lambda\}$, only the location of the first bit i_1 defines the activation condition of the SRM. Recall that the bit-flipping indices are added to any set ε_t progressively such that $i_1 < \dots < i_\lambda$. Therefore, if i_1 belongs to the second half of the codeword, the remaining bits of the set are situated there as well.

SRM can be integrated into other variations of SCF-based decoders, e.g., those of [12], [13]. Adapting the mechanism to these decoders would require minimum effort, and it can only improve their characteristics. This work focuses on SCF and DSCF- ω decoders to demonstrate the functionality.

B. Memory Structure

Fig. 2 shows a memory architecture inspired by [14] and [15] for an SCF decoder that integrates the proposed SRM. The

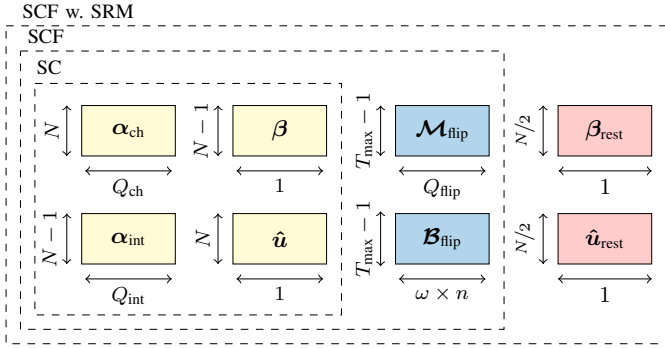


Fig. 2: Memory architecture of SCF embedding the SRM.

label indicates the content of the memory. The depth indicates the length of the data vector while the width indicates the number of bits of each entry. As depicted in Fig. 2, LLR-values and bit-flipping metrics have different quantizations. Channel LLRs use Q_{ch} bits, intermediate LLRs use Q_{int} bits and bit-flipping metrics use Q_{flip} bits. The list of bit-flipping candidates requires $(T_{\text{max}} - 1) \times \omega \times n$ bits with n being the length of the binary representation of a bit-flipping index. The remaining memory blocks are the binary vectors of single bit widths. In total, α_{ch} requires $N \times Q_{\text{ch}}$ bits, α_{int} requires $(N - 1) \times Q_{\text{int}}$ and $\mathcal{M}_{\text{flip}}$ requires $(T_{\text{max}} - 1) \times Q_{\text{flip}}$ bits. Recall that the SRM only requires partial sums and bit estimates from the LHS tree computed at the initial SC trial. Thus, the memory overhead of the SRM is N bits.

IV. EXECUTION-TIME MODEL WITH HARDWARE CONSTRAINTS

In order to estimate the latency that reflects an architectural design, we implement a model with a limited number of processing elements, denoted by P . The methodology is based on the architecture of the semi-parallel SC decoder [14].

The nodes of the SC decoding tree (Fig. 1) perform the calculations of the functions (1)–(2) with a limited number of processing elements in parallel. The latency of a single LLR calculation is considered to be of one clock cycle (CC). The vector of the partial-sums is calculated with function (5) for each node in one CC. The approach for partial-sums is valid considering simplicity of bitwise XOR operations.

The latency of a single SC pass in CCs is denoted by \mathcal{L}_{SC} , and it is given by the following equation [14]:

$$\begin{aligned} \mathcal{L}_{\text{SC}} &= \mathcal{L}_{\alpha} + \mathcal{L}_{\beta}, \\ &= \left(2N + \frac{N}{P} \cdot \log_2 \left(\frac{N}{4P} \right) \right) + (N - n - 1), \end{aligned} \quad (9)$$

where $n = \log_2(N)$, \mathcal{L}_{α} is the latency of LLR computations and \mathcal{L}_{β} is the latency of calculations of partial-sums.

The execution time of one codeword by the SCF decoder is the product of the SC pass latency and the required number of decoding trials. The required number of trials is denoted by t_{req} and the total execution time is computed as:

$$l_{\text{SCF}} = t_{\text{req}} \cdot \mathcal{L}_{\text{SC}}, \quad (10)$$

where $1 \leq t_{\text{req}} \leq T_{\text{max}}$. If $t_{\text{req}} = T_{\text{max}}$, l_{SCF} indicates the worst-case execution time and thus it is decoding latency.

The execution time being variable, the following characteristics are of interest: the average execution time, the average additional execution time and the execution-time variance. These metrics are obtained experimentally, by simulation. The average execution time \mathcal{L}_{SCF} is estimated by:

$$\mathcal{L}_{\text{SCF}} = \frac{1}{S} \sum_{s=1}^S l_{\text{SCF}}, \quad (11)$$

where S is the total number of simulated codewords. The average additional execution time $\mathcal{L}'_{\text{SCF}}$ is estimated by:

$$\mathcal{L}'_{\text{SCF}} = \frac{1}{S'} \sum_{s=1}^{S'} (l_{\text{SCF}} - \mathcal{L}_{\text{SC}}), \quad (12)$$

where $S' \leq S$ indicates the number of codewords that required more than a single SC pass to decode by SCF decoding. The execution-time variance \mathcal{V}_l is estimated by:

$$\mathcal{V}_l = \frac{1}{S' - 1} \sum_{s=1}^{S'} (l_{\text{SCF}} - \mathcal{L}_{\text{SCF}})^2. \quad (13)$$

For DSCF- ω decoders, the latency associated with the updates of the bit-flipping sets is ignored since these operations have a negligible impact on the execution time compared to SC decoding. Thus, (11)–(13) are used for the execution-time characteristics of SCF and DSCF- ω decoders.

V. SIMULATION RESULTS

A. Methodology

A simulation setup is created to analyze the effects of our proposed mechanism on SCF and DSCF- ω decoding. Random blocks of data were encoded with polar codes of $N = 1024$ for three different rates $R \in \{1/8, 1/4, 1/2\}$, and of $N = 512$ for a rate $R = 1/8$. A CRC of $r = 16$ bits with polynomial $z^{16} + z^{15} + z^2 + 1$ is applied. The polar codes are constructed for a design E_b/N_0 of 1.25 dB, 1.25 dB and 2.5 dB for length $N = 1024$ of rates $1/8$, $1/4$, and $1/2$, respectively. Polar code for $N = 512$ of rate $1/8$ is constructed for a design E_b/N_0 of 1.25 dB. Binary phase-shift keying modulation is used over an AWGN channel. Simulations were run for a minimum of $S = 10^5$ random codewords and until 10^3 frames in errors were found. DSCF- ω decoders with $\omega \in \{1, 2, 3\}$ are examined.

The number of processing elements is limited to $P = 64$ for all simulations. The DSCF- ω decoders use the hardware-friendly (8) function for metric calculations. The maximum number of trials T_{max} is set to 13 for SCF, while for DSCF- ω they are set to $T_{\text{max}} \in \{8, 51, 301\}$ for $\omega \in \{1, 2, 3\}$. The values of T_{max} were selected to achieve an error-correction performance that is close to the genie-aided decoder [7] at the target frame-error rate (FER).

We compare the decoders for $\mathcal{P}(1024, 128)$ polar code with $r = 16$ with and without the SRM in terms of error-correction performance, execution-time characteristics and memory requirements. We highlight the results of the execution-time

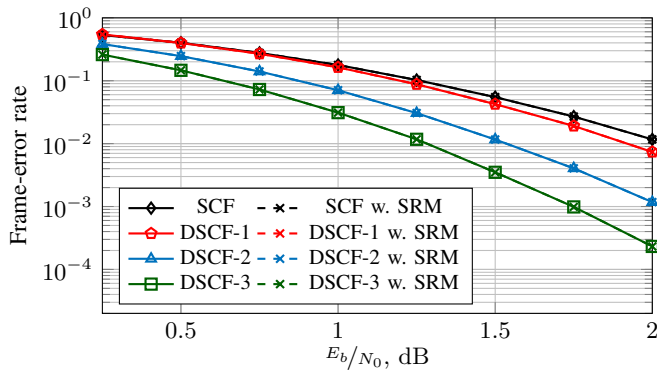


Fig. 3: Error-correction performance of SCF and DSCF- ω decoders with $\omega \in \{1, 2, 3\}$ with and without the SRM for $\mathcal{P}(1024, 128)$ polar code with $r = 16$.

characteristics of using SRM for the target FER of 10^{-2} for polar codes of different code lengths and code rates.

B. Error-Correction Performance

The error-correction performance in terms of FER for SCF and DSCF- ω decoders is shown in Fig. 3 for $\mathcal{P}(1024, 128)$ polar code. The decoders with and without the SRM are depicted in dashed and solid lines, respectively. The SCF decoder is in black, DSCF-2 is in light-blue and DSCF-3 is in light-green with unique markers.

From Fig. 3, it can be seen that the SRM does not alter the error-correction performance. This is expected and in line with the definition of the mechanism described in Section III-A. The results also agree with [7], i.e., they indicate that DSCF- ω outperforms standard SCF. The DSCF-3 decoder offers the best performance, thus the motivation to reduce the execution-time characteristics of that algorithm.

C. Execution-Time Characteristics

Fig. 4 show the average execution time of SCF and DSCF- ω decoders for $\mathcal{P}(1024, 128)$ polar code. The decoders with and without the SRM are in dashed and solid lines accordingly. The latency of SC decoding is provided for reference. From the figures, we observe that using the SRM provides greater gain to the DSCF-2 and DSCF-3 decoders throughout the FER range. We explain this by higher number of additional trials performed by the multi bit-flipping decoders in average. We also observe that DSCF-1 decoder with SRM provides the smallest reduction among the other decoders. This can be explained by low number of additional decoding attempts and low decoding latency (smallest T_{\max} among the other decoders). In Fig. 4 we can also see that at lower FER the average execution time of all decoders with and without the SRM closely approach the latency of the SC decoder.

The reduction of the execution-time characteristics are summarized in Table I for each decoder for polar codes of $N = 1024$ for various code rates. Table II shows results of $N = 512$ for $R = 1/8$ exhibiting the higher gain with the SRM. The notation for the characteristics is described in

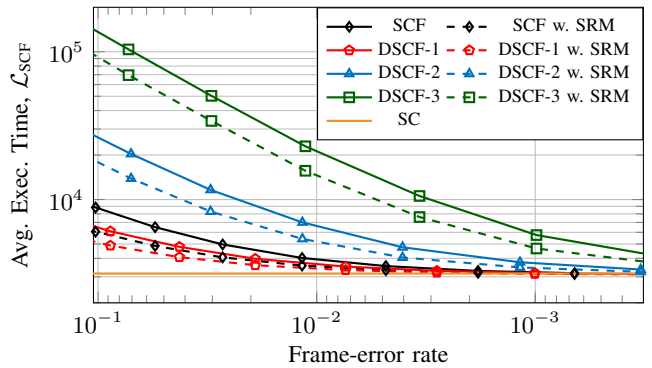


Fig. 4: Average execution time of SCF and DSCF- ω decoders with $\omega \in \{1, 2, 3\}$ with and without the SRM for $\mathcal{P}(1024, 128)$ polar code with $r = 16$. Plain SC decoder is for reference.

Section IV. The differences are denoted by Δ and presented in percent. The E_b/N_0 points for each decoder are indicated that correspond to target FER of 10^{-2} . The results provided in tables indicate the greatest gain from applying the SRM for polar code of $N = 1024$ for $R = 1/8$. Compared to the original SCF decoder, for the SCF embedding the SRM, the average execution time, the average additional execution time and the execution-time variance are reduced by 11.17%, 48.30%, and 73.50%, respectively. DSCF-1 decoder embedding SRM provides reduction of 7.57%, 43.57% and 67.28%, respectively. Highlighting the results for DSCF-3 – decoder with the strongest error-correction performance, applying the SRM provides reduction of 31.70%, 37.08% and 57.28%, respectively. Looking at results for polar codes of $N = 1024$ for higher code rates, we see that, while the reductions of the execution-time characteristics are lower, the general tendencies are preserved. Comparing results for polar codes of $N = 1024$ and $N = 512$ for $R = 1/8$, the reduction of characteristics is almost identical. Applying the SRM to DSCF-3 decoder for polar code of $N = 1024$ for $R = 1/2$ provides the reduction of 7.33%, 9.03% and 12.20%, respectively.

D. Memory Estimates

The memory is calculated as described in Section III-B, where the same quantization scheme as that of [8] is used. Hence, channel LLRs and intermediate LLRs and bit-flipping metrics are quantized by $Q_{\text{ch}} = 6$, $Q_{\text{int}} = 7$ and $Q_{\text{flip}} = 7$ bits, respectively. Out of these bits, 2 bits of Q_{ch} and Q_{int} are used for the fractional part while 3 bit are used for Q_{flip} . The memory estimates and memory overhead in percent are provided in Table III for all considered decoders. The results are provided for polar codes of different lengths, while the code rate does not affect the memory size. It can be seen from Table III that the proposed SRM leads to a memory overhead of 2.86% to 6.62%. Embedding the SRM into DSCF-3 decoder results in the smallest memory overhead compared to the other decoders, since DSCF-3 requires a much larger memory to store the list of bit-flipping candidates $\mathcal{B}_{\text{flip}}$ and the corresponding list of bit-flipping metrics $\mathcal{M}_{\text{flip}}$.

TABLE I: Reduction of the execution-time characteristics by using SRM to SCF and DSCF- ω decoders for polar codes of $N = 1024$ for various code rates at the target FER 10^{-2} .

	$\mathcal{P}(1024, 128), r = 16$					$\mathcal{P}(1024, 256), r = 16$				$\mathcal{P}(1024, 512), r = 16$			
	T_{\max}	E_b/N_0	$\Delta\mathcal{L}_{\text{SCF}}$	$\Delta\mathcal{L}'_{\text{SCF}}$	$\Delta\mathcal{V}_l$	E_b/N_0	$\Delta\mathcal{L}_{\text{SCF}}$	$\Delta\mathcal{L}'_{\text{SCF}}$	$\Delta\mathcal{V}_l$	E_b/N_0	$\Delta\mathcal{L}_{\text{SCF}}$	$\Delta\mathcal{L}'_{\text{SCF}}$	$\Delta\mathcal{V}_l$
SCF	13	2.0	11.17	48.30	73.50	1.875	9.00	44.68	69.15	2.375	6.54	37.44	59.71
DSCF-1	8	1.875	7.57	43.57	67.28	1.75	5.01	33.33	50.87	2.25	2.95	22.04	32.35
DSCF-2	51	1.5	22.73	40.71	63.26	1.44	14.74	27.60	41.74	2.00	6.96	13.83	19.00
DSCF-3	301	1.25	31.70	37.08	57.28	1.25	19.09	22.57	34.78	1.875	7.33	9.03	12.20
		in dB	Δ in %			in dB	Δ in %			in dB	Δ in %		

TABLE II: Reduction of the execution-time characteristics by using SRM to SCF and DSCF- ω decoders for polar codes of $N = 512$ for $R = 1/8$ at the target FER 10^{-2} .

	$\mathcal{P}(512, 64), r = 16$				
	T_{\max}	E_b/N_0	$\Delta\mathcal{L}_{\text{SCF}}$	$\Delta\mathcal{L}'_{\text{SCF}}$	$\Delta\mathcal{V}_l$
SCF	13	2.625	10.36	47.49	72.27
DSCF-1	8	2.625	6.03	43.93	67.94
DSCF-2	51	2.0	24.01	40.52	63.08
DSCF-3	301	1.75	32.33	37.59	58.67
		in dB	Δ in %		

VI. CONCLUSION

In this work, we proposed simplified restart mechanism (SRM), a mechanism that reduces the execution-time characteristics of SCF and DSCF- ω decoders by starting trials beyond the initial one from the middle of the decoding process if the flipping index falls into the right-hand side of the decoding tree. The mechanism requires to store a small amount of results from the initial SC pass after the left-hand side of the tree has been visited. We showed the minor modifications required to use it in a DSCF- ω decoder. The proposed mechanism can be integrated to other SCF-based decoding algorithms, does not affect the error-correction performance, and works with any code length and rate. For a DSCF-3 decoder for polar code of length 1024 bits, the average execution time, the average additional execution time and the execution-time variance were shown to be reduced by 31%, 37% and 57%, respectively, at the cost of a 3.9% memory overhead.

ACKNOWLEDGEMENT

The authors want to thank Tannaz Kalatian for her initial work on the topic. Work supported by NSERC Discovery Grant #651824.

REFERENCES

- [1] E. Arkan, "Channel polarization: A method for constructing capacity-achieving codes for symmetric binary-input memoryless channels," *IEEE Trans. Inf. Theory*, no. 7, Jul. 2009.
- [2] I. Tal and A. Vardy, "List decoding of polar codes," *IEEE Trans. Inf. Theory*, Mar. 2015.
- [3] 3GPP, "NR; Multiplexing and channel coding," Tech. Rep. TS 38.212, Jan. 2018, Release 16.5. [Online]. Available: <http://www.3gpp.org/DynaReport/38-series.htm>
- [4] F. Ercan, C. Condo *et al.*, "On error-correction performance and implementation of polar code list decoders for 5G," in *Ann. Allerton Conf. on Commun., Control, and Comput. (Allerton)*, Oct. 2017.

TABLE III: Memory estimates and memory overhead of decoders caused by SRM for polar codes of $N \in \{1024, 512\}$.

Polar code with $N = 1024$				
	T_{\max}	no SRM, bits	w. SRM, bits	mem. incr., %
SCF	13	15556	16580	6.58
DSCF-1	8	15471	16495	6.62
DSCF-2	51	16702	17726	6.13
DSCF-3	301	26452	27476	3.87
Polar code with $N = 512$				
	T_{\max}	no SRM, bits	w. SRM, bits	mem. incr., %
SCF	13	7864	8376	6.51
DSCF-1	8	7784	8296	6.58
DSCF-2	51	8922	9434	5.74
DSCF-3	301	17872	18384	2.86

- [5] O. Afisiadis, A. Balatsoukas-Stimming, and A. Burg, "A low-complexity improved successive cancellation decoder for polar codes," in *Asilomar Conf. on Signals, Syst., and Comput. (ACSSC)*, Nov. 2014.
- [6] P. Giard, A. Balatsoukas-Stimming *et al.*, "POLARBEAR: A 28-nm FD-SOI ASIC for decoding of polar codes," *IEEE J. Emerg. Sel. Topics Circuits Syst.*, vol. 7, no. 4, Dec. 2017.
- [7] L. Chandesaris, V. Savin, and D. Declercq, "Dynamic-SCFlip decoding of polar codes," *IEEE Trans. Commun.*, no. 6, Jun. 2018.
- [8] F. Ercan, T. Tonnellier *et al.*, "Practical dynamic SC-Flip polar decoders: Algorithm and implementation," *IEEE Trans. Signal Process.*, Sep. 2020.
- [9] I. Sagitov and P. Giard, "An early-stopping mechanism for DSCF decoding of polar codes," in *IEEE Int. Workshop on Signal Process. Syst. (SiPS)*, Sep. 2020.
- [10] I. Tal and A. Vardy, "How to construct polar codes," *IEEE Trans. Inf. Theory*, no. 10, Oct. 2013.
- [11] F. Ercan, T. Tonnellier *et al.*, "Simplified dynamic SC-flip polar decoding," in *IEEE Int. Conf. on Acoustics, Speech, and Signal Process. (ICASSP)*, May 2020.
- [12] P. Giard and A. Burg, "Fast-SSC-Flip decoding of polar codes," in *IEEE Wireless Commun. and Netw. Conf. (WCNC)*, Apr. 2018.
- [13] F. Ercan, C. Condo, and S. Hashemi, "Partitioned successive-cancellation flip decoding of polar codes," in *IEEE Int. Conf. on Commun. (ICC)*, May 2018.
- [14] C. Leroux, A. Raymond *et al.*, "A semi-parallel successive-cancellation decoder for polar codes," *IEEE Trans. Signal Process.*, Oct. 2012.
- [15] S. Hashemi, C. Condo, and W. Gross, "Fast and flexible successive-cancellation list decoders for polar codes," *IEEE Trans. Signal Process.*, Nov. 2017.